
VLCACHE: Computing 2% Vision Tokens and Reusing 98% for Vision–Language Inference

Shengling Qin^{1*} Hao Yu^{1*} Chenxin Wu^{2*} Zheng Li¹
 Yizhong Cao¹ Zhengyang Zhuge¹ Yuxin Zhou¹ Wentao Yao¹ Yi Zhang¹
 Zhengheng Wang² Shuai Bai¹ Jianwei Zhang^{1†} Junyang Lin¹

¹Qwen Team, Alibaba Inc.
²TairKVCache Team, Alibaba Cloud

Abstract

This paper presents VLCache, a cache reuse framework that exploits both Key-Value (KV) cache and encoder cache from prior multimodal inputs to eliminate costly recomputation when the same multimodal inputs recur. Unlike previous heuristic approaches, we formally identify the cumulative reuse error effect and demonstrate how to minimize the non-prefix cache reuse error effectively. We further analyze the varying importance of model layers and propose a dynamic, layer-aware recomputation strategy to balance accuracy and efficiency. Experimental results show that VLCache achieves an accuracy on par with full recomputation, while requiring only 2–5% of the tokens to compute, yielding 1.2x–16x TTFT speedups. We develop an experimental implementation of the proposed VLCache pipeline based on SGLang, enabling significantly faster inference in practical deployments.

1 Introduction

The Vision-Language Model (VLM) has emerged as a fundamental paradigm for visual question answering and multimodal understanding. With a Vision Transformer (ViT) [5, 8] as the visual embedding backbone, and a Large Language Model (LLM) [1, 10, 12] as the main reasoning module, the VLM shows remarkable performance in complex tasks, such as visual reasoning, referring expression comprehension, and multimodal dialogue.

To speed up the inference of language models, engineers leverage the Key-Value (KV) cache computed for a previous request in future requests to skip time-consuming computation. This attention mechanism requires an exact prefix match for lossless cache reuse and token generation. Considering that the prefix match requirement is not always met, several position-independent reuse schemes, including CacheBlend [14], MPIC [16] and KVShare [13], have emerged to address this problem. Those methods enable the reuse of the KV cache across different requests, even when initial token sequences differ, thereby eliminating the dependency on shared prefixes. To partially correct the reuse error, these algorithms will recompute part of the tokens at designated positions. Then the problem becomes deciding the recomputation rate and the position of recomputed tokens.

However, these heuristic schemes show significant issues in defining the *importance* of the vision tokens, which is the basis of selecting the top ones for recomputation. For CacheBlend and KVShare, the KV cache distance or the attention score distance between the reused and recomputed tokens is used to decide the importance of each token. Although effective on some occasions, this local

*Equal contribution.

†Corresponding author.

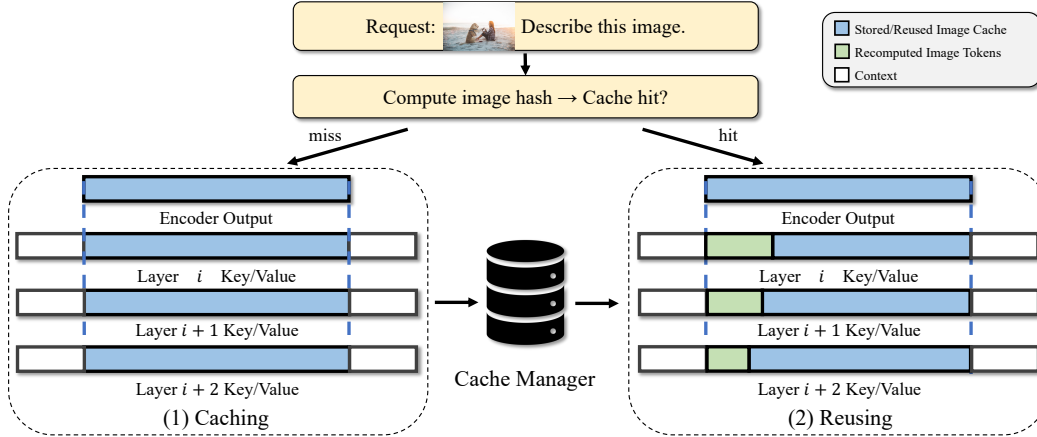


Figure 1: Overview of VLCACHE. Both the KV cache and encoder cache are stored and will be reused in future requests, with selective recomputation in the KV cache to ensure accuracy.

information at the layer level cannot accurately tell the importance of the token. We find that, when evaluating the attention outputs, the token with the greatest distance is often not the most important one. For MPIC, the recomputation budget is allocated to several earlier tokens of each reused cache chunk. The effectiveness of MPIC relies on the *attention sink* effect, where the initial tokens in the prompt—typically the system prompt—attract high attention. In our setting, however, this effect does not occur because the reused vision tokens do not function as a system prompt.

To address these issues, we have an in-depth investigation into reuse errors in VLMs. We identify the *cumulative error effect* on VL cache reuse, which propagates the initial error to later tokens. We argue that this cumulative error is a key reason why *recomputing the initial image tokens* can effectively mitigate performance degradation. In addition, we observe that different transformer layers contribute unevenly to the final model output. Building on this insight, we further analyze the *layer-wise importance diversity* in VLMs. Based on the error cumulative effect we have discovered, we propose a dynamic algorithm that allocates an optimal per-layer recomputation rate given a fixed overall recomputation budget.

Integrating these findings, we propose VLCACHE, an end-to-end vision token KV cache reuse pipeline. VLCache stores the output of the vision encoder for each image patch along with the corresponding KV cache. When the same image is encountered again in a subsequent request, VLCache bypasses the vision encoder computation entirely and directly reuses the stored encoder cache and KV cache. To preserve output accuracy, VLCache selectively recomputes a layer-dependent fraction of the initial image tokens at each LLM layer. Compared with previous methods, extensive experiments demonstrate that VLCache offers two key advantages: higher acceleration and better accuracy. With only 2-5% of vision tokens recomputed, VLCache achieves near-lossless accuracy. We integrate the VLCache pipeline into the SGLang framework, significantly reducing the *Time-To-First-Token (TTFT)*. Depending on the model architecture and the length of the input image tokens, VLCache yields 1.2x to 16x TTFT speedups.

2 Preliminaries

2.1 KV Cache for LLMs

Vision language models (VLMs) [2, 9, 3] have demonstrated human-level capabilities in understanding and generating multimodal content. State-of-the-art VLMs typically employ a Vision Transformer (ViT) [4, 5] as the visual encoder, which is then integrated into a large-scale pre-training large language model (LLM) backbone [1, 10, 11]. In general, LLMs are built on the neural structure of Transformers [8], which requires a computational cost quadratic to the input sequence’s length and makes long sequence inference intractable. To mitigate this inefficiency, the auto-regressive decoding LLMs support Key-Value (KV) caches, i.e., to cache the previous context’s intermediate key and value states in memory. KV caches can avoid redundant computation of previous tokens, thus

expediting the inference process. Building upon KV cache, the prefix caching [7, 17] mechanism will retain the KV cache of fixed or shared prefix sequences (such as system prompts or task instructions). This further reduces computation overhead by allowing the model to skip processing the repeated prefix entirely during inference.

2.2 Position-Independent KV Cache Reuse

The prefix cache mechanism stipulates that a new request can only reuse KV cached content if its initial segment (i.e., prefix) exactly matches an existing cached sequence. While this strict matching criterion ensures output accuracy, it introduces a significant efficiency bottleneck. Position-independent KV Cache reuse, on the other hand, allows for reusing the pre-cached KV Cache at different locations, thereby achieving higher flexibility. To maintain accuracy after reusing position-independent KV Cache, it is necessary to recompute part of the token’s KV Cache. To determine the token indices that need to be recomputed, different researchers have proposed various methods. CacheBlend [14] will first calculate the distances of the first three layers of KV Cache, record the farthest token index, and then recompute these tokens in the remaining layers. EPIC [6] and MPIC [16] will recompute the initial tokens of each chunk. Depending on the deviation of the attention map, KVShare [13] will selectively recompute critical tokens during the prefilling and decoding stages. However, all those methods lack both an in-depth analysis of how reused tokens affect the decoding stage and a systematic investigation into the impact of different model layers on the final output.

3 Observations

3.1 Cumulative Reuse Error Effect

The self-attention mechanism implies that the output of a token is influenced by its surrounding context. In causal language models, where each token attends to itself and all preceding tokens, the output depends on itself and its prefix. When a multimodal input is reused in a new request, its context differs from the original one—this discrepancy, known as *prefix mismatch*, leads to what we call *reuse error* in the KV cache. For causal language models, the reuse error of a token consists of two components: the *self reuse error* and the *propagated error* from previously reused tokens. The propagated error from previous tokens to the current token can then be expressed as:

$$e_k^{prop} = \sum_{i=1}^{k-1} e_{(i,k)}^{prop}, \quad (1)$$

where $e_{(i,k)}^{prop}$ represents the propagated error from the reused token at position i to position k . Thus, the total reuse error for token k is given by:

$$e_k^{total} = e_k^{self} + e_k^{prop} \quad (2)$$

$$= e_k^{self} + \sum_{i=1}^{k-1} e_{(i,k)}^{prop} \quad (3)$$

$$= e_k^{self} + e_{(1,k)}^{prop} + \dots + e_{(k-2,k)}^{prop} + e_{(k-1,k)}^{prop}. \quad (4)$$

Therefore, the ‘accuracy’ of a reused token is affected by all previously reused tokens, while it, in turn, influences all subsequent tokens. We refer to this phenomenon as *reuse error propagation*. This property introduces positional weighting among tokens and serves as the theoretical foundation for designing an efficient recomputation token selection strategy.

To validate the propagation of the reuse error, we conduct several experiments shown in Fig. 2. Using two representative image inputs, we measure each token’s attention output error when its key/value states are reused rather than recomputed, and compare per-token error norms under different recomputation ratios throughout the generation sequence. In both examples, the propagation pattern is clear: early reused tokens introduce errors that persist and accumulate, yielding larger error norms for later tokens. Selectively recomputing early tokens (e.g., 10% or 30%) significantly suppresses downstream accumulation, as early recomputation cancels a large portion of the upstream error. These

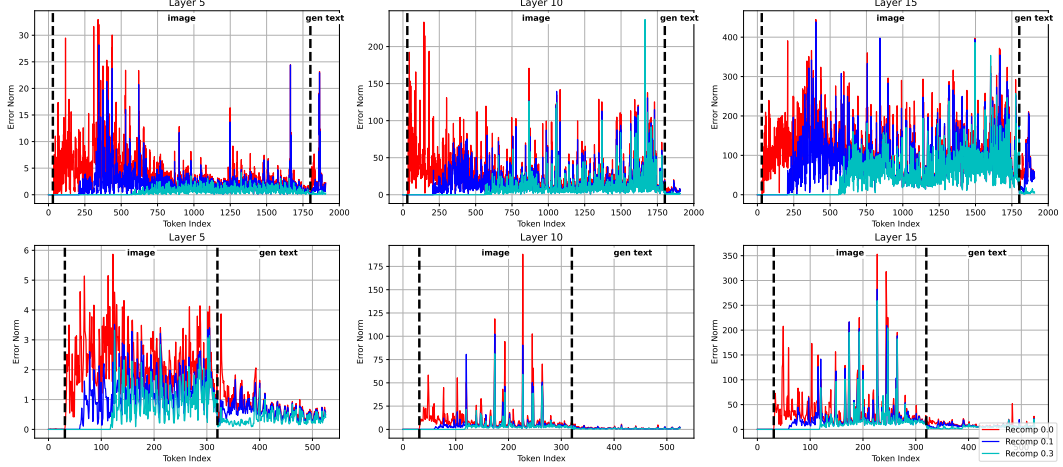


Figure 2: The reuse error of earlier token recomputation for two image examples. Earlier token recomputation cancels out more reuse errors and slows down the error accumulation at later generated tokens, leading to better accuracy.

findings directly support our theoretical claim that reuse error induces a positional weighting effect and show that prioritizing earlier tokens for recomputation offers disproportionately large accuracy gains.

3.2 Layer-wise Importance Difference

As mentioned above, different model layers exert distinct influences on the output. To validate this hypothesis, we conducted an empirical experiment on Qwen2.5-VL-7B. Specifically, we select 20 samples each from the MMMU-Pro [15] Standard & Vision dataset used as experimental subjects. The entire experimental procedure consists of the following three phases:

- Constructing the KV cache with a replacement prompt. For each sample, we keep the image input unchanged and replace the original question prompt with a semantically unrelated or neutral alternative prompt (e.g., ‘Please describe this image’). In this setting, we perform a full forward pass and cache the image-related KV cache.
- Obtaining the original output as the baseline. Next, we conduct standard decoding with the original prompt, recording the output logits and corresponding text.
- Reuse KV cache and measure errors. Finally, we combine the original question prompt and the text generated via standard decoding as input. During inference, we inject the image KV cache generated from the substituted prompt (i.e., a ‘mismatched’ KV cache) into all layers, while recomputing the KV cache for only the top 10% & 20% & 30% of image tokens in a single layer. We record the logits of the decoding text and compute the MSE loss between them and the logits produced by the original model.

The loss curve is shown in Fig 3. Compared to directly reusing the KV cache, applying different recomputation ratios across layers leads to varying degrees of MSE loss reduction for the decoding text. These results show that using the same recomputation ratio across all layers is *sub-optimal*, as some more sensitive layers should have a higher recomputation ratio, while some layers should not even recompute image tokens at all.

4 Algorithm

4.1 VLCache: Reuse and Dynamic Recomputation

Basic Algorithm Based on the above observations, we design the VLCache algorithm illustrated in Fig. 1, which reuses most vision tokens while selectively recomputing a small subset of important ones. VLCache operates as a plugin within the standard inference pipeline. Upon receiving a

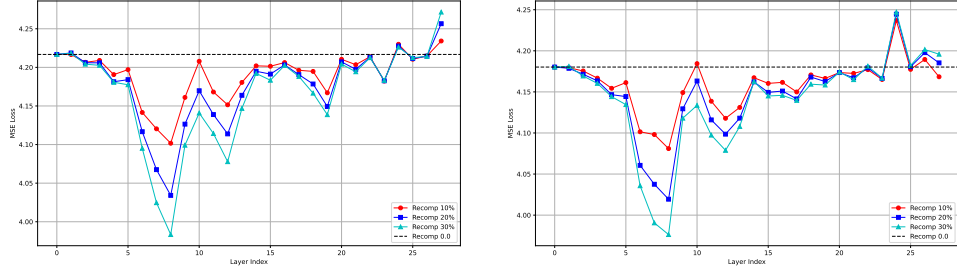


Figure 3: MSE loss between the logits of the generated text and those produced by the original model (with correct KV cache), when recomputing the top 10%, 20%, and 30% of image tokens, evaluated on the MMMU-Pro Standard (left) and MMMU-Pro Vision (right) datasets.

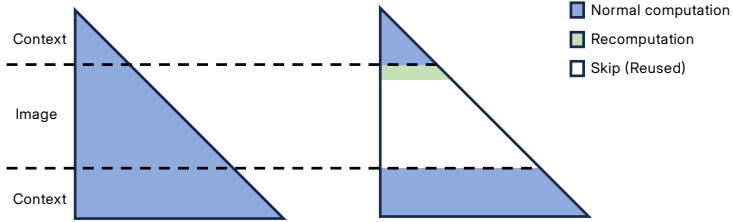


Figure 4: Full attention computation (left) v.s. VLCache partial attention computation (right). VLCache skips a large portion of attention operations and forms contiguous computation regions, which is hardware-friendly.

request, it first computes a hash of the input image. For cache misses, normal prefilling is performed and both the encoder cache and KV cache are stored in the backend KVCache store. For cache hits, the stored encoder and KV caches are retrieved and reused. We directly reuse most image tokens and only recompute a small set of early tokens, with the recomputation ratio denoted as r . The query tokens and the selected tokens for recomputation are concatenated to form the actual model input. For reused tokens, all associated computations—including attention and MLP—will be skipped, which determines the acceleration. An example of attention skipping is shown in Fig. 4. The resulting attention computation regions become contiguous, making the kernel execution more hardware-friendly.

Dynamic Recomputation As previously discussed, a key challenge lies in accurately determining the proportion of tokens to recompute for each layer. To address this, we propose an adaptive search strategy, i.e., to allocate a higher recomputation ratio to layers that are more sensitive to output quality, while applying a more aggressive KV cache reuse policy to less sensitive layers.

Given a proxy dataset D , we follow the experimental procedure outlined in Section 3.2. First, we generate the mismatched KV cache (i.e., using a substituted prompt) and reuse it across all layers. Next, for each layer, we evaluate the MSE loss of the decoding text logits corresponding to the original model and recompute a fixed proportion of image tokens in that layer, i.e.,

$$\mathcal{S}_i(r) = \mathbb{E}_{(x,y) \in \mathcal{D}} \text{MSE}(\mathbf{z}^{\text{orig}}, \mathbf{z}_{i,r}^{\text{reuse}}), \quad (5)$$

where $\mathcal{S}_i(r)$ is the layer i sensitivity score with recomputation rate r (e.g., $r=0.002, 0.004, \dots, 0.300$). \mathbf{z}^{orig} is the logits produced by the original model using correct KV cache. $\mathbf{z}_{i,r}^{\text{reuse}}$ represents the logits where the mismatched key-value cache is reused across all layers, and only in the i -th layer the first r tokens will be recomputed.

After obtaining the sensitivity scores for each layer, given a target total recomputation ratio P_{tar} , we minimize the sum of sensitivity scores across all layers, subject to the constraint that the per-layer recomputation ratio is non-increasing with depth (i.e., monotonically decreasing or constant across

layers). That is

$$\underset{\{r_i\}_{i=1}^L}{\text{minimize}} \quad \sum_{\ell=1}^L \mathcal{S}_i(r) \quad (6)$$

$$\text{subject to} \quad \sum_{i=1}^L r_i \leq P_{\text{tar}}, \quad (7)$$

$$r_1 \geq r_2 \geq \dots \geq r_L \geq 0, \quad (8)$$

$$r_i \in \{0.002, 0.004, \dots, 0.300\}, \quad \forall i \in \{1, \dots, L\}. \quad (9)$$

Given a set of distinct target parameters, we can dynamically generate multiple choices, demonstrating remarkable flexibility.

Since the selected ranks are discrete, this optimization problem is inherently an integer programming problem. To address it, we propose a simple greedy algorithm for an approximate solution. Notably, we adopt a simplifying assumption: the sensitivity of a given layer depends only on its own recomputation strategy and is independent of the ranks chosen for other layers. Although this greedy algorithm does not guarantee a globally optimal configuration, exhaustively searching over all possible combinations to find the exact global minimum is computationally prohibitive. In contrast, our approximate greedy approach dramatically accelerates the search process. As we will demonstrate in subsequent experiments, the adaptive configurations obtained via this greedy strategy achieve strong performance across diverse model architectures and a wide range of tasks.

Notably, to ensure the validity of acceleration, the token recomputation rate must be monotonically non-increasing across layers, i.e., $r_i \leq r_{i-1}$ for all layers. This constraint arises from VLCache’s core mechanism: it reuses hidden states of retained tokens from upper layers and skips their corresponding attention and MLP computations in subsequent layers. If a deeper layer were assigned a higher recomputation rate than the shallow layer, it would require recomputing hidden states for tokens that were not retained (and thus not available for reuse) by the shallow layer. This will violate the reuse assumption and introduce redundant computation, which directly contradicts the acceleration objective.

4.2 SGLang Integration of VLCache

For evaluation, we implement the proposed VLCache pipeline as a prototype based on the SGLang framework. Our integration introduces two key modifications: (1) skipping ViT computation via hash-based image embedding caching, and (2) skipping attention and MLP computation through per-image adaptive recomputation with fine-grained KV cache reuse.

For the ViT encoder, we implement request-level embedding reuse based on content hashing. Upon receiving a multimodal request, SGLang computes a global hash over the concatenated pixel values of all input images. If this hash matches a previously processed request, the precomputed image embeddings are retrieved from a distributed key-value store which is Tair KVCache Store in practice, entirely bypassing ViT computation. Otherwise, embeddings are computed and stored for future reuse.

To support image-level KV cache reuse, each image in a request is assigned an individual hash based on its pixel content. These per-image hashes enable fine-grained identification of reused visual content across varying contexts, enabling modular cache management. We store the KV cache before rotary position embedding (RoPE) is applied. Building on this, we implement adaptive recomputation in different attention layers using *Block Sparse Attention*. At each layer, a recompute ratio r determines the fraction of tokens to recompute per image. For an image with T tokens, only the first $\lfloor r \cdot T \rfloor$ tokens undergo full attention computation; the remainder reuse their KV states from prior executions, indexed by the corresponding image hash. In practice, we construct a *computation mask* at each layer to identify which tokens require computation or not. This binary mask is used to index into the input hidden states, extracting only the subset of tokens designated for fresh processing. The selected tokens are then passed through RoPE and fed into the attention kernel for computation.

These features are seamlessly integrated into SGLang’s execution engine. The system transparently accelerates VLM inference, enabling efficient deployment of long-context multimodal workloads.

Table 1: Speedup for Qwen3-VL-8B

Configuration	1K		3K		5K		10K		20K	
	TTFT	Speedup								
Origin	0.392	1.00x	1.176	1.00x	1.993	1.00x	4.087	1.00x	8.784	1.00x
w/o ViT	0.286	1.37x	0.962	1.22x	1.631	1.22x	3.428	1.19x	7.565	1.16x
Static ($r=0.3$)	0.249	1.57x	0.794	1.48x	1.306	1.53x	2.592	1.58x	5.341	1.64x
Static ($r=0.2$)	0.229	1.71x	0.752	1.56x	1.235	1.61x	2.428	1.68x	4.945	1.78x
Static ($r=0.1$)	0.230	1.70x	0.720	1.63x	1.208	1.65x	2.361	1.73x	4.666	1.88x
Static ($r=0.0$)	0.227	1.73x	0.692	1.70x	1.133	1.76x	2.206	1.85x	4.430	1.98x
Dynamic ($\bar{r} = 0.035$)	0.253	1.55x	0.750	1.57x	1.222	1.63x	2.408	1.70x	4.823	1.82x
Dynamic ($\bar{r} = 0.025$)	0.259	1.51x	0.728	1.62x	1.258	1.58x	2.438	1.68x	4.714	1.86x

Table 2: Speedup for Qwen3-VL-32B

Configuration	1K		3K		5K		10K		20K	
	TTFT	Speedup	TTFT	Speedup	TTFT	Speedup	TTFT	Speedup	TTFT	Speedup
Origin	0.772	1.00x	2.501	1.00x	4.186	1.00x	8.927	1.00x	20.279	1.00x
w/o ViT	0.701	1.10x	2.218	1.13x	3.761	1.11x	8.078	1.11x	18.549	1.09x
Static ($r=0.3$)	0.423	1.83x	1.337	1.87x	2.183	1.92x	4.335	2.06x	9.102	2.23x
Static ($r=0.2$)	0.368	2.10x	1.098	2.28x	1.901	2.20x	3.787	2.36x	7.794	2.60x
Static ($r=0.1$)	0.330	2.34x	0.963	2.60x	1.551	2.70x	2.984	2.99x	6.099	3.32x
Static ($r=0.0$)	0.306	2.52x	0.792	3.16x	1.313	3.19x	2.522	3.54x	5.144	3.94x
Dynamic ($\bar{r} = 0.035$)	0.393	1.96x	0.995	2.51x	1.643	2.55x	3.136	2.85x	6.399	3.17x
Dynamic ($\bar{r} = 0.025$)	0.383	2.02x	1.023	2.44x	1.651	2.54x	3.160	2.83x	6.375	3.18x

5 Experiments and Discussion

5.1 Acceleration of VLCache

We evaluate the effectiveness of VLCache in reducing *Time to First Token (TTFT)* on Qwen3-VL-8B and Qwen3-VL-32B using an NVIDIA H20-3e GPU. Each input prompt follows the format:

<text><image_1><image_2>...<image_n>,

where the number of images varies across requests, simulating realistic multimodal workloads. Experiments are conducted with varying total input lengths (including both text and image tokens) under the following four configurations:

- Origin: Baseline setup with full computation;
- w/o ViT: Skip ViT computation by reusing cached image embeddings;
- Static Recompute: Skip ViT using cached image embeddings, and skip attention and MLP computation with a uniform recompute ratio r applied across all layers;
- Dynamic Recompute: Skip ViT using cached image embeddings, and skip attention and MLP computation with layer-adaptive recompute ratios. The average recompute ratio is denoted as \bar{r} .

To measure the sensitivity of a specific layer, we randomly select 40 samples from the training set to construct an auxiliary dataset D . The specific recomputation ratio for each model can be viewed in our code.

Table 1 - 2 present the detailed TTFT acceleration results. Here, the text remains fixed at 20 tokens, and the terms like ‘1K’, ‘3K’ refer to the length of the image tokens. For Qwen3-VL series models, we observe substantial speedups of up to 3.9x. The acceleration is predominantly attributable to KV cache reuse, as a result of the more efficient ViT module architecture in the model. The speedup becomes more pronounced as the number of image tokens increases, since KV cache reuse effectively reduces the computationally intensive attention operation with $O(n^2)$ complexity. To minimize the recomputation rate, we employ a dynamic recomputation scheme, which introduces a small overhead but maintains significant speedup, especially for longer input sequences.

Table 3: Accuracy Preservation for Qwen3-VL-8B

Dataset	$r = 0.0$	$\bar{r} = 0.025$	$\bar{r} = 0.035$	$r = 0.1$	$r = 0.2$	$r = 0.3$	$r = 1.0$
MMMU-VAL	67.44	67.33	67.00	68.00	67.22	66.56	66.33
MMMU-Pro-Standard	53.82	54.28	54.68	54.05	53.53	54.51	54.10
MMMU-Pro-Vision	53.12	53.29	53.93	52.49	53.29	52.60	52.14
MathVista-MINI	77.00	77.20	77.00	77.60	77.60	77.70	77.80
HallusionBench	58.97	60.17	60.28	60.45	59.18	60.59	61.78
MBench-DEV-CN-V11	84.13	84.37	84.29	84.06	84.37	84.75	85.53
MBench-DEV-EN-V11	85.14	85.91	85.84	85.45	85.91	86.15	85.91
RealWorldQA	71.13	71.76	71.76	71.76	72.03	71.37	70.98
AI2D-TEST	85.27	84.75	85.01	85.20	84.68	85.49	85.43
ChartQA-TEST	83.60	84.44	84.44	84.44	84.08	84.12	84.24
DocVQA-VAL	94.84	95.15	95.15	95.08	95.13	95.14	95.09
Mean	74.04	74.42	74.49	74.42	74.27	74.45	74.48

Table 4: Accuracy Preservation for Qwen3-VL-32B

Dataset	$r = 0.0$	$\bar{r} = 0.025$	$\bar{r} = 0.035$	$r = 0.1$	$r = 0.2$	$r = 0.3$	$r = 1.0$
MMMU-VAL	73.78	74.44	73.44	74.11	73.67	74.78	73.00
MMMU-Pro-Standard	64.57	63.93	65.20	63.76	65.09	63.70	63.18
MMMU-Pro-Vision	61.01	61.21	62.77	62.60	62.02	62.43	61.68
MathVista-MINI	82.90	82.90	82.90	83.30	82.70	83.00	82.10
HallusionBench	62.53	63.52	62.90	62.43	61.81	63.48	64.13
MBench-DEV-CN-V11	88.70	89.01	89.40	89.09	89.01	88.62	88.70
MBench-DEV-EN-V11	89.32	89.09	89.09	89.32	89.09	89.55	89.47
RealWorldQA	79.35	80.65	79.87	80.26	79.08	78.95	78.69
AI2D-TEST	88.21	88.70	88.83	88.99	88.99	88.80	88.89
ChartQA-TEST	83.00	83.64	83.56	83.96	84.48	84.32	86.92
DocVQA-VAL	95.83	95.78	95.84	95.80	95.87	95.70	95.87
Mean	79.01	79.35	79.44	79.42	79.26	79.39	79.33

5.2 Accuracy Preservation of VLCache

We assess the near-lossless performance of VLCache across a broad suite of vision-language benchmarks, covering general visual question answering, visual mathematics, OCR-based tasks, and hallucinations. The experiments are conducted in the following manner:

- Extract the images from the dataset, and pair each image with a relevant query to construct an auxiliary prompt;
- Construct the encoder cache and KV cache pool by input the auxiliary prompt;
- Send the formal prompt and evaluate the model response.

The results are shown in Table 3 - Table 4. For example, across the datasets in Table 3, VLCache maintains accuracy extremely well even at low recomputation rates. For example, at $r = 0.1$, most datasets show accuracy values nearly identical to the $r = 1.0$ (full-recompute) baseline. Datasets such as MMMU-VAL, MathVista-MINI, RealWorldQA, ChartQA-TEST, and DocVQA-VAL all remain within roughly 0–1 percentage points of their full-recompute accuracy. More challenging benchmarks, such as HallusionBench or MBench-DEV-CN-V11, display similarly tight accuracy preservation, with changes typically under 1–2 points.

Besides, our dynamic KV-cache recomputation strategy achieves remarkable accuracy preservation across diverse multimodal benchmarks—even at very low recomputation rates. Notably, the mean accuracy peaks at $\bar{r} = 0.035$ (74.49). This advantage stems from our layer-wise dynamic allocation of recomputation budget: rather than uniformly recompute tokens across layers (as in static schemes), our method preferentially targets layers and tokens where cache staleness most harms model output—yielding higher fidelity at lower cost.

Table 5: Performance comparison of our method and prior SOTA on Qwen3-VL-8B. ‘Cache’ uses KV-cache distance for matching (CacheBlend), while ‘Attn.’ uses attention-map-based matching (KVShare).

Metric	$r = 0.1$			$r = 0.2$			$r = 0.3$		
	Ours	Cache	Attn.	Ours	Cache	Attn.	Ours	Cache	Attn.
MMMU-VAL	68.00	68.89	68.45	67.22	67.56	67.20	66.56	65.78	65.95
MMMU-Pro-Standard	54.05	54.45	54.22	53.53	53.29	53.30	54.51	54.45	55.08
MMMU-Pro-Vision	52.49	53.41	52.10	53.29	52.31	52.65	52.60	53.70	52.02
MathVista-MINI	77.60	76.40	75.95	77.60	76.70	77.15	77.70	76.90	76.08
MathVision	60.45	58.72	58.20	59.18	60.09	59.70	60.59	59.29	58.40
MBench-DEV-CN-V11	84.06	84.13	83.55	84.37	84.91	84.10	84.75	84.52	83.95
MBench-DEV-EN-V11	85.45	84.91	84.30	85.91	85.45	85.85	86.15	85.72	85.10
RealWorldQA	71.76	71.37	70.80	72.03	70.98	71.10	71.37	71.50	70.65
AI2D-TEST	85.20	85.98	84.85	84.68	85.10	84.20	85.49	85.17	84.45
ChartQA-TEST	84.44	83.64	83.10	84.08	83.44	82.95	84.12	83.44	83.80
DocVQA-VAL	95.08	95.17	94.55	95.13	95.19	94.60	95.14	95.18	94.50
Mean	74.42	74.28	73.64	74.27	74.09	73.89	74.45	74.15	73.63

Overall, the tables demonstrate that VLCache can maintain 99% accuracy at low recomputation rates, with accuracy steadily increasing as r grows, and that dynamic recomputation provides better performance compared to static approaches.

5.3 Comparisons with Other SOTA Methods

We conduct comparison experiments between our proposed VLCache and two state-of-the-art baselines, i.e., CacheBlend [14] and KVShare [13] under identical hyperparameter settings. Without employing our dynamic strategy, we adopt a uniform recomputation rate across all layers—specifically 10%, 20%, and 30%. As shown in Table 5, VLCache consistently outperforms both baselines at every recomputation rate, demonstrating its effectiveness, robustness, and the validity of the underlying *cumulative reuse error effect*.

6 Conclusion

In this work, we propose VLCache, a cache reuse scheme designed to accelerate the prefill stage of VLMs while preserving inference accuracy. VLCache provides a holistic design that integrates algorithmic optimizations and system-level implementations, achieving significant acceleration without compromising accuracy. It demonstrates substantial speedup over standard VLM inference, especially in scenarios where multiple queries are paired with a same set of images to become overlapping requests. Following this work, future explorations could investigate extending cache reuse to similar visual inputs, enabling broader applicability across diverse multi-query or multi-image tasks.

References

- [1] Jinze Bai, Shuai Bai, Yunfei Chu, Zeyu Cui, Kai Dang, Xiaodong Deng, Yang Fan, Wenbin Ge, Yu Han, Fei Huang, Binyuan Hui, Luo Ji, Mei Li, Junyang Lin, Runji Lin, Dayiheng Liu, Gao Liu, Chengqiang Lu, Keming Lu, Jianxin Ma, Rui Men, Xingzhang Ren, Xuancheng Ren, Chuanqi Tan, Sinan Tan, Jianhong Tu, Peng Wang, Shijie Wang, Wei Wang, Shengguang Wu, Benfeng Xu, Jin Xu, An Yang, Hao Yang, Jian Yang, Shusheng Yang, Yang Yao, Bowen Yu, Hongyi Yuan, Zheng Yuan, Jianwei Zhang, Xingxuan Zhang, Yichang Zhang, Zhenru Zhang, Chang Zhou, Jingren Zhou, Xiaohuan Zhou, and Tianhang Zhu. Qwen technical report. *arXiv preprint arXiv:2309.16609*, 2023.
- [2] Jinze Bai, Shuai Bai, Shusheng Yang, Shijie Wang, Sinan Tan, Peng Wang, Junyang Lin, Chang Zhou, and Jingren Zhou. Qwen-vl: A versatile vision-language model for understanding, localization, text reading, and beyond. *arXiv preprint arXiv:2308.12966*, 2023.
- [3] Shuai Bai, Keqin Chen, Xuejing Liu, Jialin Wang, Wenbin Ge, Sibo Song, Kai Dang, Peng Wang, Shijie Wang, Jun Tang, Humen Zhong, Yuanzhi Zhu, Mingkun Yang, Zhaohai Li, Jianqiang Wan, Pengfei Wang, Wei Ding, Zheren Fu, Yiheng Xu, Jiabo Ye, Xi Zhang, Tianbao Xie, Zesen Cheng, Hang Zhang, Zhibo Yang, Haiyang Xu, and Junyang Lin. Qwen2.5-vl technical report. *arXiv preprint arXiv:2502.13923*, 2025.
- [4] Mostafa Dehghani, Basil Mustafa, Josip Djolonga, Jonathan Heek, Matthias Minderer, Mathilde Caron, Andreas Steiner, Joan Puigcerver, Robert Geirhos, Ibrahim M Alabdulmohsin, Avital Oliver, Piotr Padlewski, Alexey Gritsenko, Mario Lucic, and Neil Houlsby. Patch n' pack: Navit, a vision transformer for any aspect ratio and resolution. In *Advances in Neural Information Processing Systems*, volume 36, pages 2252–2274, 2023.
- [5] Alexey Dosovitskiy, Lucas Beyer, Alexander Kolesnikov, Dirk Weissenborn, Xiaohua Zhai, Thomas Unterthiner, Mostafa Dehghani, Matthias Minderer, Georg Heigold, Sylvain Gelly, Jakob Uszkoreit, and Neil Houlsby. An image is worth 16x16 words: Transformers for image recognition at scale. In *International Conference on Learning Representations (ICLR)*, 2021.
- [6] Junhao Hu, Wenrui Huang, Weidong Wang, Haoyi Wang, tiancheng hu, zhang qin, Hao Feng, Xusheng Chen, Yizhou Shan, and Tao Xie. EPIC: Efficient position-independent caching for serving large language models. In *Proceedings of the 42nd International Conference on Machine Learning*, 2025.
- [7] Woosuk Kwon, Zhuohan Li, Siyuan Zhuang, Ying Sheng, Lianmin Zheng, Cody Hao Yu, Joseph E. Gonzalez, Hao Zhang, and Ion Stoica. Efficient memory management for large language model serving with pagedattention. In *Proceedings of the ACM SIGOPS 29th Symposium on Operating Systems Principles*, 2023.
- [8] Ashish Vaswani, Noam Shazeer, Niki Parmar, Jakob Uszkoreit, Llion Jones, Aidan N Gomez, Łukasz Kaiser, and Illia Polosukhin. Attention is all you need. In *Advances in Neural Information Processing Systems 30*, volume 30, pages 5998–6008, 2017.
- [9] Peng Wang, Shuai Bai, Sinan Tan, Shijie Wang, Zhihao Fan, Jinze Bai, Keqin Chen, Xuejing Liu, Jialin Wang, Wenbin Ge, Yang Fan, Kai Dang, Mengfei Du, Xuancheng Ren, Rui Men, Dayiheng Liu, Chang Zhou, Jingren Zhou, and Junyang Lin. Qwen2-vl: Enhancing vision-language model's perception of the world at any resolution. *arXiv preprint arXiv:2409.12191*, 2024.
- [10] An Yang, Baosong Yang, Binyuan Hui, Bo Zheng, Bowen Yu, Chang Zhou, Chengpeng Li, Chengyuan Li, Dayiheng Liu, Fei Huang, Guanting Dong, Haoran Wei, Huan Lin, Jialong Tang, Jialin Wang, Jian Yang, Jianhong Tu, Jianwei Zhang, Jianxin Ma, Jin Xu, Jingren Zhou, Jinze Bai, Jinzheng He, Junyang Lin, Kai Dang, Keming Lu, Keqin Chen, Kexin Yang, Mei Li, Mingfeng Xue, Na Ni, Pei Zhang, Peng Wang, Ru Peng, Rui Men, Ruize Gao, Runji Lin, Shijie Wang, Shuai Bai, Sinan Tan, Tianhang Zhu, Tianhao Li, Tianyu Liu, Wenbin Ge, Xiaodong Deng, Xiaohuan Zhou, Xingzhang Ren, Xinyu Zhang, Xipin Wei, Xuancheng Ren, Yang Fan, Yang Yao, Yichang Zhang, Yu Wan, Yunfei Chu, Yuqiong Liu, Zeyu Cui, Zhenru Zhang, and Zhihao Fan. Qwen2 technical report. *arXiv preprint arXiv:2407.10671*, 2024.

- [11] An Yang, Baosong Yang, Beichen Zhang, Binyuan Hui, Bo Zheng, Bowen Yu, Chengyuan Li, Dayiheng Liu, Fei Huang, Haoran Wei, Huan Lin, Jian Yang, Jianhong Tu, Jianwei Zhang, Jianxin Yang, Jiaxi Yang, Jingren Zhou, Junyang Lin, Kai Dang, Keming Lu, Keqin Bao, Kexin Yang, Le Yu, Mei Li, Mingfeng Xue, Pei Zhang, Qin Zhu, Rui Men, Runji Lin, Tianhao Li, Tingyu Xia, Xingzhang Ren, Xuancheng Ren, Yang Fan, Yang Su, Yichang Zhang, Yu Wan, Yuqiong Liu, Zeyu Cui, Zhenru Zhang, and Zihan Qiu. Qwen2.5 technical report. *arXiv preprint arXiv:2412.15115*, 2024.
- [12] An Yang, Anfeng Li, Baosong Yang, Beichen Zhang, Binyuan Hui, Bo Zheng, Bowen Yu, Chang Gao, Chengan Huang, Chenxu Lv, Chujie Zheng, Dayiheng Liu, Fan Zhou, Fei Huang, Feng Hu, Hao Ge, Haoran Wei, Huan Lin, Jialong Tang, Jian Yang, Jianhong Tu, Jianwei Zhang, Jianxin Yang, Jiaxi Yang, Jing Zhou, Jingren Zhou, Junyang Lin, Kai Dang, Keqin Bao, Kexin Yang, Le Yu, Lianghao Deng, Mei Li, Mingfeng Xue, Mingze Li, Pei Zhang, Peng Wang, Qin Zhu, Rui Men, Ruize Gao, Shixuan Liu, Shuang Luo, Tianhao Li, Tianyi Tang, Wenbiao Yin, Xingzhang Ren, Xinyu Wang, Xinyu Zhang, Xuancheng Ren, Yang Fan, Yang Su, Yichang Zhang, Yingqi Zhang, Yu Wan, Yuqiong Liu, Zekun Wang, Zeyu Cui, Zhenru Zhang, Zhipeng Zhou, and Zihan Qiu. Qwen3 technical report. *arXiv preprint arXiv:2505.09388*, 2025.
- [13] Huan Yang, Renji Zhang, Mingzhe Huang, Weijun Wang, Yin Tang, Yuanchun Li, Yunxin Liu, and Deyu Zhang. KVShare: An llm service system with efficient and effective multi-tenant kv cache reuse. *arXiv preprint arXiv:2503.16525*, 2025.
- [14] Jiayi Yao, Hanchen Li, Yuhan Liu, Siddhant Ray, Yihua Cheng, Qizheng Zhang, Kuntai Du, Shan Lu, and Junchen Jiang. CacheBlend: Fast large language model serving for rag with cached knowledge fusion. In *Proceedings of the Twentieth European Conference on Computer Systems*, page 94–109, 2025.
- [15] Xiang Yue, Tianyu Zheng, Yuansheng Ni, Yubo Wang, Kai Zhang, Shengbang Tong, Yuxuan Sun, Botao Yu, Ge Zhang, Huan Sun, Yu Su, Wenhui Chen, and Graham Neubig. MMMU-pro: A more robust multi-discipline multimodal understanding benchmark. In *Proceedings of the 63rd Annual Meeting of the Association for Computational Linguistics (Volume 1: Long Papers)*, pages 15134–15186, 2025.
- [16] Shiju Zhao, Junhao Hu, Rongxiao Huang, Jiaqi Zheng, and Guihai Chen. MPIC: Position-independent multimodal context caching system for efficient mllm serving. *arXiv preprint arXiv:2502.01960*, 2025.
- [17] Lianmin Zheng, Liangsheng Yin, Zhiqiang Xie, Chuyue Sun, Jeff Huang, Cody Hao Yu, Shiyi Cao, Christos Kozyrakis, Ion Stoica, Joseph E. Gonzalez, Clark Barrett, and Ying Sheng. Sglang: Efficient execution of structured language model programs. In *Advances in Neural Information Processing Systems*, volume 37, pages 62557–62583, 2024.

A Additional Results

A.1 Comparing Recomputing Earlier v.s. Later Tokens

To determine which strategy yields lower reuse error, we compare allocating the recomputation budget to earlier versus later tokens. As shown in Fig. 5, recomputing *earlier tokens* significantly reduces the accumulated error. In contrast, recomputing later tokens provides only limited improvement, since early-stage errors have already propagated through the sequence, resulting in substantially higher overall error.

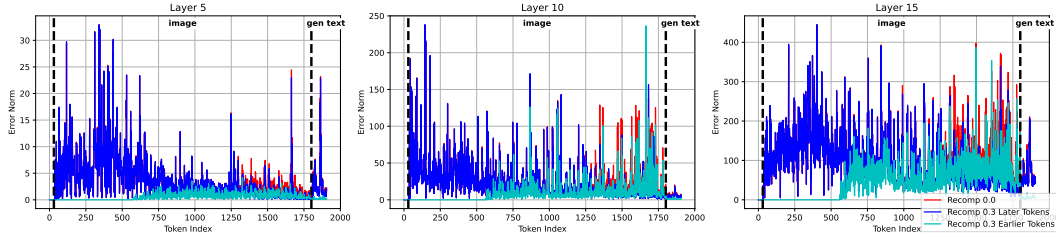


Figure 5: The reuse error of recomputing earlier tokens versus later tokens. Earlier token recomputation cancels out more reuse error and slows down the error propagation, leading to significantly lower error in generated texts.

A.2 Additional Results on Qwen2.5-VL Models

To further demonstrate the effectiveness of our method, we also conducted relevant experiments on Qwen2.5VL-7B and Qwen2.5VL-32B. The speed and accuracy results are shown in the Table 6 - Table 9 below.

We can draw the same conclusion. As the recomputation rate increases from $r = 0.0$ toward $r = 1.0$, most datasets show a gradual upward trend. For instance, MMMU-VAL rises from 56.78 to 58.00, MathVision from 25.20 to 25.39, and RealWorldQA from 68.50 to 69.02. While a few datasets exhibit small oscillations (e.g., MMMU-Pro-Vision, AI2D-TEST), the overall average accuracy improves as more tokens are recomputed.

Moreover, the results highlight that the layer-wise dynamic KV cache recomputation scheme achieves higher accuracy than static recomputation at the same recomputation rate. This advantage is especially visible at intermediate rates (e.g., $r = 0.1$ – 0.3), where dynamic recomputation yields accuracy that is notably closer to the full-recompute values.

A.3 Additional Results on Qwen3-VL Models

To further demonstrate the effectiveness of our method, we evaluate the inference-time efficiency and accuracy trade-offs of various vision compression strategies on Qwen3-VL-30B-A3B model.

As shown in Table 10, though the overall acceleration is lower, we have consistently achieved a 20%–80% TTFT acceleration. Crucially, Table 11 demonstrates that aggressive compression incurs minimal accuracy degradation, i.e., VLCache with $\bar{r} = 0.035$ outperforms the baseline in mean accuracy (76.52 v.s. 76.47). This further supports the robustness of our approach. Overall, these results reveal a highly favorable Pareto frontier, i.e., up to 1.79 \times faster TTFT with no loss, and sometimes improvement in accuracy.

Table 6: Speedup for Qwen2.5-VL-7B

Configuration	1.4K		3.6K		5K		10K		20K	
	TTFT	Speedup	TTFT	Speedup	TTFT	Speedup	TTFT	Speedup	TTFT	Speedup
Origin	0.635	1.00x	2.631	1.00x	4.398	1.00x	16.160	1.00x	62.750	1.00x
w/o ViT	0.322	1.97x	0.985	2.67x	1.334	3.30x	2.693	6.00x	6.251	10.04x
Static ($r=0.3$)	0.251	2.53x	0.722	3.64x	0.987	4.46x	2.006	8.06x	4.402	14.25x
Static ($r=0.2$)	0.231	2.75x	0.673	3.91x	0.936	4.70x	1.877	8.61x	4.054	15.48x
Static ($r=0.1$)	0.216	2.94x	0.612	4.30x	0.844	5.21x	1.740	9.29x	3.847	16.31x
Static ($r=0.0$)	0.210	3.02x	0.606	4.34x	0.825	5.33x	1.626	9.94x	3.701	16.95x
Dynamic ($\bar{r} = 0.1$)	0.255	2.49x	0.712	3.70x	0.957	4.60x	1.912	8.45x	4.130	15.19x
Dynamic ($\bar{r} = 0.05$)	0.232	2.74x	0.699	3.76x	0.879	5.00x	1.885	8.57x	3.966	15.82x

Table 7: Accuracy Preservation for Qwen2.5-VL-7B

Dataset	$r = 0.0$	$\bar{r} = 0.01$	$\bar{r} = 0.02$	$\bar{r} = 0.05$	$r = 0.1$	$\bar{r} = 0.1$	$r = 0.2$	$r = 0.3$	$r = 1.0$
MMMU-VAL	56.78	56.78	57.11	57.78	57.00	57.33	57.33	57.44	58.00
MMMU-Pro-Standard	41.16	41.50	41.56	41.56	40.87	41.10	41.10	40.69	40.87
MMMU-Pro-Vision	33.24	34.45	34.91	34.91	34.68	35.90	35.09	36.99	36.99
MathVista-MINI	67.00	67.20	65.80	66.90	67.40	67.60	68.80	68.50	68.40
MathVision	25.20	24.51	25.66	26.05	25.82	26.35	25.56	26.22	25.39
HallusionBench	50.54	50.46	51.24	50.37	50.15	50.66	50.76	50.81	53.13
MBench-DEV-CN-V11	80.88	81.04	80.88	80.96	81.04	80.88	81.11	81.35	82.20
MBench-DEV-EN-V11	83.20	83.13	83.28	83.13	83.05	82.89	82.89	83.13	84.13
RealWorldQA	68.50	68.50	68.76	68.37	68.50	68.63	68.24	68.50	69.02
AI2D-TEST	84.26	84.13	84.23	84.26	84.07	84.20	84.03	84.20	84.13
ChartQA-TEST	86.08	85.92	86.24	86.20	86.40	86.44	86.24	86.40	87.40
DocVQA-VAL	94.61	94.61	94.60	94.58	94.60	94.63	94.58	94.43	94.74
Mean	64.29	64.35	64.52	64.59	64.47	64.72	64.64	64.88	65.37

Table 8: Speedup for Qwen2.5-VL-32B

Configuration	1.4K		3.6K		5K		10K		20K	
	TTFT	Speedup	TTFT	Speedup	TTFT	Speedup	TTFT	Speedup	TTFT	Speedup
Origin	1.176	1.00x	3.961	1.00x	6.525	1.00x	20.110	1.00x	70.570	1.00x
w/o ViT	0.873	1.35x	2.342	1.69x	3.226	2.02x	6.865	2.93x	15.351	4.60x
Static ($r=0.3$)	0.503	2.34x	1.303	3.04x	1.777	3.67x	3.494	5.76x	7.649	9.23x
Static ($r=0.2$)	0.457	2.57x	1.073	3.69x	1.488	4.39x	2.969	6.77x	6.308	11.19x
Static ($r=0.1$)	0.375	3.14x	0.944	4.20x	1.275	5.12x	2.707	7.43x	5.444	12.96x
Static ($r=0.0$)	0.325	3.62x	0.620	6.39x	0.820	7.96x	1.905	10.56x	4.181	16.88x
Dynamic ($\bar{r} = 0.04$)	0.391	3.01x	0.929	4.26x	1.181	5.52x	2.443	8.23x	5.406	13.05x
Dynamic ($\bar{r} = 0.02$)	0.397	2.96x	0.920	4.31x	1.201	5.43x	2.469	8.14x	5.286	13.35x

Table 9: Accuracy Preservation for Qwen2.5-VL-32B

Dataset	$r = 0.0$	$\bar{r} = 0.02$	$\bar{r} = 0.04$	$r = 0.1$	$r = 0.2$	$r = 0.3$	$r = 1.0$
MMMU-VAL	66.56	67.00	67.89	67.89	66.67	66.78	67.00
MMMU-Pro-Standard	51.50	52.25	52.08	51.85	51.91	51.62	51.91
MMMU-Pro-Vision	45.26	46.65	47.28	45.95	45.78	46.53	46.59
MathVista-MINI	75.70	75.30	75.60	75.00	74.20	74.10	74.30
MathVision	38.55	38.95	38.45	39.61	39.87	39.77	39.41
HallusionBench	57.20	56.78	57.21	57.55	57.46	56.41	57.17
MBench-DEV-CN-V11	85.14	85.53	85.29	85.22	85.06	85.22	85.45
MBench-DEV-EN-V11	86.30	86.46	86.53	86.22	86.84	86.76	86.61
RealWorldQA	69.54	70.20	70.46	69.54	69.67	69.41	70.85
AI2D-TEST	85.33	85.65	85.30	85.78	85.85	85.88	85.52
ChartQA-TEST	68.92	69.72	69.44	69.64	70.20	70.92	74.60
DocVQA-VAL	92.52	92.55	92.54	92.73	92.44	92.50	92.68
Mean	68.54	68.92	69.01	68.92	68.83	68.83	69.34

Table 10: Speedup for Qwen3-VL-30B-A3B

Configuration	1K		3K		5K		10K		20K	
	TTFT	Speedup								
Origin	0.350	1.00x	1.052	1.00x	1.802	1.00x	3.758	1.00x	8.172	1.09x
w/o ViT	0.322	1.09x	0.815	1.29x	1.418	1.27x	3.006	1.25x	6.931	1.18x
Static ($r=0.3$)	0.314	1.11x	0.756	1.39x	1.233	1.46x	2.447	1.54x	4.997	1.64x
Static ($r=0.2$)	0.299	1.17x	0.750	1.40x	1.245	1.45x	2.369	1.59x	4.804	1.70x
Static ($r=0.1$)	0.283	1.24x	0.752	1.40x	1.280	1.41x	2.462	1.53x	4.736	1.73x
Static ($r=0.0$)	0.327	1.07x	0.747	1.41x	1.226	1.76x	2.385	1.58x	4.697	1.74x
Dynamic ($\bar{r} = 0.035$)	0.310	1.13x	0.761	1.38x	1.215	1.47x	2.325	1.62x	4.562	1.79x
Dynamic ($\bar{r} = 0.025$)	0.317	1.10x	0.785	1.34x	1.216	1.48x	2.311	1.63x	4.572	1.79x

Table 11: Accuracy Preservation for Qwen3-VL-30B-A3B

Dataset	$r = 0.0$	$\bar{r} = 0.025$	$\bar{r} = 0.035$	$r = 0.1$	$r = 0.2$	$r = 0.3$	$r = 1.0$
MMMU-VAL	71.00	69.33	70.00	69.56	69.44	70.56	70.89
MMMU-Pro-Standard	59.83	60.75	60.06	61.27	61.56	60.40	60.46
MMMU-Pro-Vision	53.35	53.53	54.51	54.05	53.35	54.57	55.49
MathVista-MINI	78.10	79.80	80.10	79.70	79.60	79.90	78.20
HallusionBench	60.61	60.75	61.07	60.75	60.65	61.80	62.20
MBench-DEV-CN-V11	87.15	86.53	87.31	87.00	86.61	87.23	86.76
MBench-DEV-EN-V11	87.38	87.62	88.24	87.54	87.85	88.08	88.47
RealWorldQA	74.12	73.99	75.16	74.51	73.99	73.73	73.33
AI2D-TEST	85.40	85.98	85.04	85.69	85.40	85.49	84.81
ChartQA-TEST	85.60	85.76	85.72	85.60	85.84	86.04	85.96
DocVQA-VAL	94.47	94.36	94.48	94.32	94.36	94.41	94.59
Mean	76.09	76.22	76.52	76.36	76.24	76.56	76.47